A practical method for seismic retrofit of tall buildings with supplemental damping

Sarven Akcelyan[1], Dimitrios G. Lignos[2]

[1] Ph.D., Course Lecturer, Department of Civil Engineering and Applied Mechanics, McGill University - Montréal, QC, Canada.

[2] Associate Professor, Department of Architecture, Civil and Environmental Engineering, École Polytechnique Fédérale de Lausanne (EPFL) - Lausanne, Switzerland.

ABSTRACT

Current simplified design methods for buildings with supplemental damping devices are mainly based on single-degree-freedom (SDF) shear-models. Common errors of such methods are attributed to the linearization of nonlinear damping and stiffness, higher building vibration modes and flexural deformations that may be ignored in the damper design phase. In tall buildings, dampers are typically placed at certain levels only, leading to an irregular vertical damping distribution along the building height. To overcome the above-mentioned challenges, a practical multi-degree-of-freedom (MDF) performance curve tool is developed for the design of tall buildings with dampers. The method first utilizes the SDF performance curve method to design and distribute dampers along the building height for a broad range of design parameters. Then, it conducts an intermediate evaluation through response history analysis based on simplified MDF models. The emphasis is placed on the use of bilinear oil dampers for seismic retrofit applications. Dampers are represented mathematically with a Maxwell model, which accounts for the stiffness characteristics of a bilinear oil damper. Guidance is provided on the development of the MDF performance curves with simplified flexural-shear beam models. A parametric study is carried out based on a broad range of damping properties and vertical damping distribution methods. An existing 40-story steel building representing typical 1970s construction in North America is used as a benchmark in this case. It is shown that the proposed tool allows for a reliable computation of story-based engineering demand parameters for a range of available seismic retrofit design solutions.

Keywords: Supplemental damping, tall buildings, seismic retrofit, bilinear oil dampers, performance curves.

INTRODUCTION

Supplemental damping devices have been implemented in buildings to minimize the seismic effects in prospective and existing designs [1]. To this end, simplified design methods, such as linear analysis procedures (LAPs), were developed and adopted in the design practice [2]. The LAPs can be easily utilized along with a code-based design spectrum by assuming linearized single-degree-of-freedom (SDF) systems. However, LAPs possess errors, which in many instances, may not be negligible [3]. Simplified design methodologies for buildings with supplemental damping devices do not accurately represent challenges common to high-rise buildings. Dampers are not always designed to be present in all stories (e.g., tall buildings) [4; 5]. The damping localization in few stories results in nonclassical damping, thereby resulting in EDP prediction errors. Disregarding the flexural deformations in simplified formulations also results into errors [5-7]. Flexural deformations in tall steel moment-resting frame (MRF) buildings may reduce the damper efficiency and increase the seismic demands in the upper stories of a building. Tall buildings are prone to higher mode effects that are not properly represented by simplified linear static procedures.

Nonlinear response history analysis (NRHA) is the most reliable method for tall building seismic evaluation. However, NRHA is not practical for optimizing the damper design along the building height when iterative design procedures are employed. For this purpose, Guo and Christopoulos [8] proposed a simplified design tool to reduce the associated computational cost. It comprises equivalent SDF systems (P-Spectra). Albeit the computational efficiency, it is still challenging to accurately predict the story-based EDPs along the building height due to the SDF simplified assumptions.

This paper presents an MDF performance curve method, which is a practical design tool for buildings equipped with supplemental damping devices. The development of the MDF performance curves is illustrated in a step-by-step process. A benchmark 40-story steel MRF building designed in 1970s is employed for this purpose. The building is retrofitted with bilinear oil dampers.

PROTOTYPE TALL BUILDING

The tall building is representative of 1970s construction in the West Coast of the US. The use of space MRFs were common in tall buildings of the time [9]. The building is designed according to UBC 1973 [10], in which the strong-column-weak-beam ratio was not a design requirement. Figure 1a shows the plan view of a 40-story steel building to be retrofitted. Figure 1b and 1c show the elevation views of the building in the X- and Y-loading directions, respectively. The typical story height is 3m (10 ft). The columns comprise built-up box sections, while beams consist of wide-flange (W-) shapes. Two dimensional nonlinear analysis models are developed in *OpenSees* [11] for assessing the building seismic performance in the two orthogonal directions according to ASCE 41-13 [12]. The fundamental periods of the building are around 5.30 sec in both loading directions based on conventional eigenvalue analysis. Steel columns employ stocky cross sections (depth-to-thickness ratios of 5.7 to 26.7). Therefore, they are not expected to experience local buckling induced softening [13; 14]. Thus, steel columns are modeled with force-based elements having five-integration points and assigned a cross-section discretized into fiber elements [15]. . Steel beams are modeled as elastic elements with concentrated plasticity in their ends based on the modified Ibarra-Medina-Krawinkler model [16; 17]. This model is assigned input parameters for pre-Northridge beam-to-column connections developed by Lignos et al. [18]. Panel zones are modeled based on the Krawinkler model [19] based on the approach discussed in Gupta and Krawinkler [20]. Two earthquake hazard levels corresponding to a probability of exceedance of 20% in 50 years (BSE-1E) and 5% in 50 years (BSE-2E) are considered according to ASCE/SEI [12] . Forty ground motions are selected and scaled to be compatible with the uniform hazard spectrum of BSE-1E and BSE-2E levels based on site-specific seismic hazard analysis. results from NRHA reveal that 29 and 13 out of 40 ground motions lead to structural collapse in the X- and Y-loading directions, respectively. End columns in bottom stories in the X-loading direction attain their squash load due to the transient component of seismic loading. Hence the prototype building shall be retrofitted. Further details regarding the design and seismic assessment of the building can be found in Akcelyan [21].
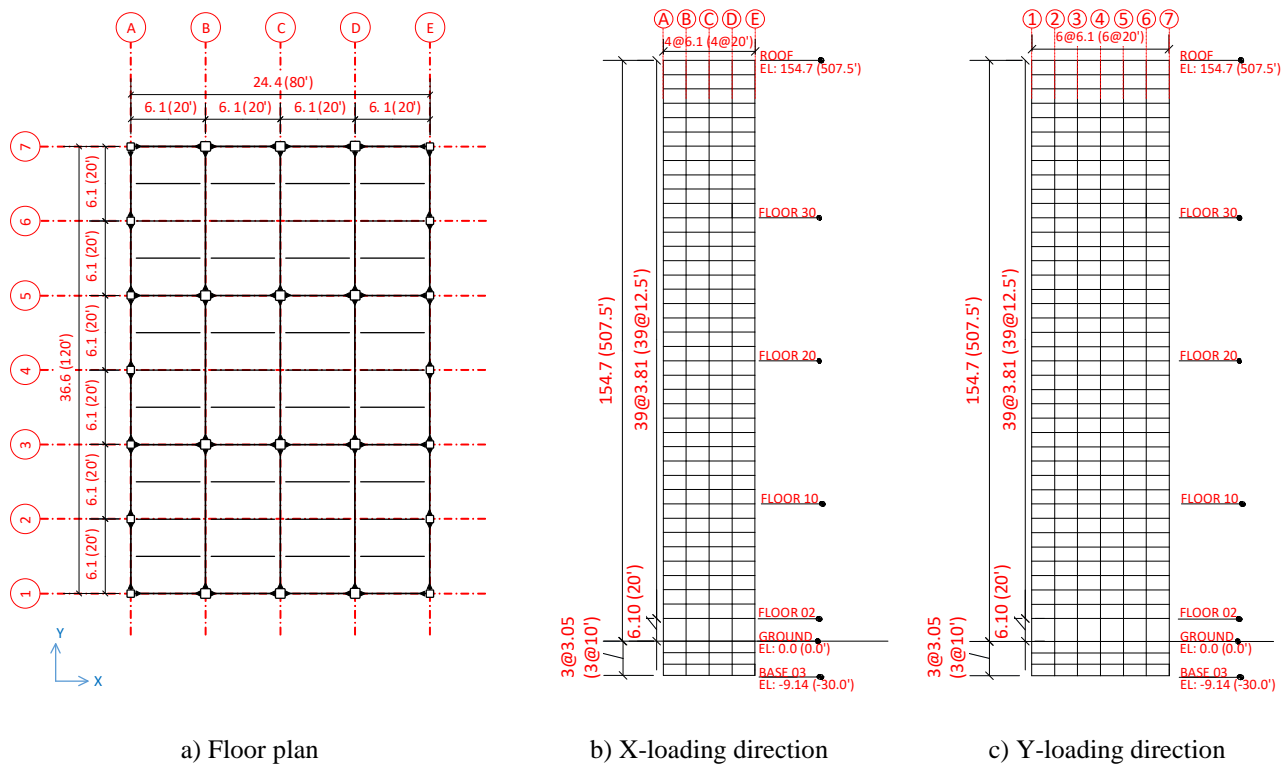

| a) Floor plan | b) X-loading direction | c) Y-loading direction |

Figure 1. Plan view and elevation of the 40-story prototype steel building; dimensions in meters (inches in parenthesis)

CONSTRUCTION OF MDF PERFORMANCE CURVES

The generation of MDF performance curves comprises five steps. In the first one, preliminary selection of key parameters shall be conducted by using the SDF performance curve method (Figure 2a). The SDF design is then transformed to an MDF one by distributing vertically the damping parameters along the building height (Figure 2b). In turn, simplified flexural-shear beam models are generated by assigning the building properties and dampers within each story (Figure 2b). In the fourth step, NRHA is conducted with the developed MDF model. The model is subjected to the selected ground motion set. Representative seismic EDPs are then computed as shown in Figure 2d. This procedure is repeated with a range of design parameters. Finally, MDF

performance curves are generated. These are shown in Figure 2e. Details of each step and generation of MDF performance curves for the 40-story archetype building are presented in the subsequent sections.
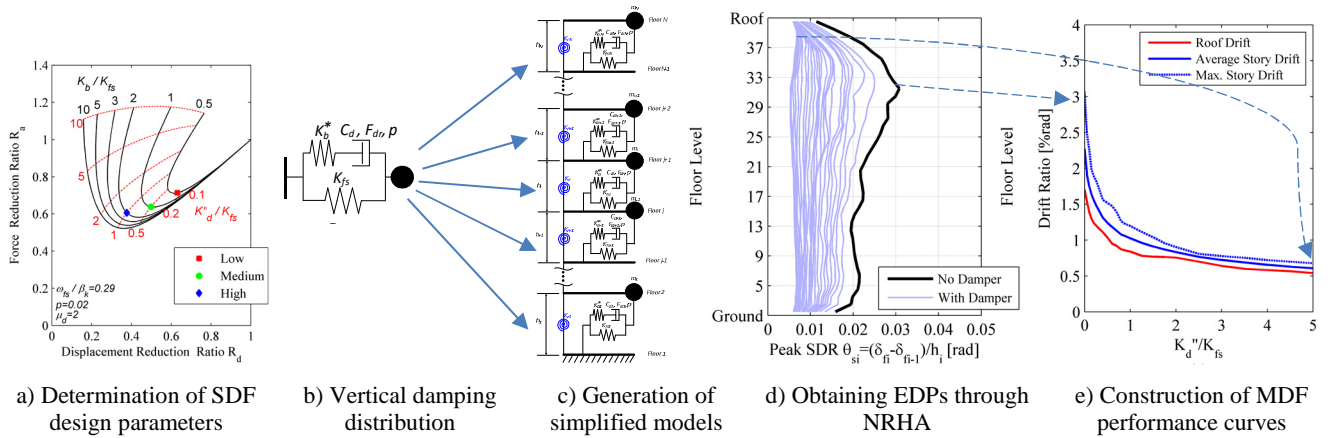

| a) Determination of SDF design parameters | b) Vertical damping distribution | c) Generation of simplified models | d) Obtaining EDPs through NRHA | e) Construction of MDF performance curves |

Figure 2. Steps to construct MDF performance curves.

Performance Curves Method

The performance curves method is a linear static procedure, which serves as a practical tool to design buildings with dampers. [22-24] . Figure 3 shows the graphical representation of the main SDF parameters used in the design of buildings equipped with bilinear oil dampers. Particularly, Figure 3a shows the SDF representation of a bilinear oil damper model. An oil damper contains low viscosity oil with a relief mechanism, which suppresses the force demand after a certain limit, hence it demonstrates a bilinear force-velocity relation.(F_d - $ú_d$) [25; 26]. This relation can be expressed mathematically as follows.

$$F_d(t) = \begin{cases} C_d ú_d(t), & |F_d(t)| \le F_{dr} \\ \text{sgn}(ú_d(t))\left(F_{dr} + pC_d\left(|ú_d(t)| - ú_{dr}\right)\right), & |F_d(t)| > F_{dr} \end{cases} \quad (1)$$

in which, C_d is the initial damping coefficient, p is the post relief damping coefficient ratio; F_{dr} and $ú_{dr}$ are the relief force and velocity of the bilinear oil damper, respectively. As shown in Figure 3a, assuming a sinusoidal displacement excitation $u_d(t) = u_{d0}\sin(\omega t)$, the peak damper force F_{d0} can be expressed as follows,

$$F_{d0} = \left(p + \frac{1-p}{\mu_d}\right)C_d\omega u_{d0}, \quad \mu_d = \frac{ú_{d0}}{ú_{dr}} = \frac{\omega u_{d0}}{ú_{dr}} \quad (2)$$

in which, u_{d0} and ω are the peak displacement amplitude and the circular frequency of the sinusoidal excitation, respectively. The peak damper velocity ratio, μ_d, is defined as the ratio of the maximum velocity demand over the damper relief velocity. In fact, the damper assembly is not only a pure dashpot model. It also includes the axial stiffnesses of the supporting brace, K_b, and of the damper portion, K_d. For simplicity, these can be combined into an equivalent damper stiffness, K_b^*, as illustrated in Figure 3b. The damper assembly can be idealized as a Maxwell model. This generates a storage stiffness, K_a'. Figure 3c represents the building with dampers as an SDF system. This comprises a shear frame in parallel with a Maxwell bilinear oil damper. In this figure, K_{fs} represents the shear stiffness of the SDF system without dampers (i.e., shear stiffness of the frame building). The total lateral stiffness of the building should consider a flexural stiffness contribution. However, lamping it within a shear frame assumption leads to erroneous results, particularly for tall buildings. Hence, the flexural stiffness is considered more rigorously as discussed below. Figure 3 shows the graphical definition of dynamic stiffnesses, such as the loss (K_d'', K_a'', K'') and storage stiffnesses (K_d', K_a', K'). By analyzing these three systems and computing the effects of K_d''/K_{fs} and K_b/K_{fs} ratios on the SDF system response, performance curves for buildings with bilinear oil dampers are developed. Figure 4a illustrates the variation of effective damping and period. Figure 4b shows the displacement-force reduction (R_d and R_a) with respect to the frame without dampers. Note that, the performance curves are functions of case specific parameters, such as the shear frame frequency, $\omega_{fs}=2\pi/T_{fs}$, the stiffness-to-damping coefficient ratio of the internal damper, β_k, the post-relief damping coefficient ratio, p and the peak damper velocity ratio μ_d. Therefore, the performance curves shown in Figure 4 are applicable for the Y-loading direction of the prototype building. Available damper sizes can aid the initial value selection of the considered parameters. For instance, for the building under consideration the fundamental shear frame period, T_{fs}= 4.8sec. The damper properties are assumed to be, $\beta_k = 4.5$, p=0.02, $\mu_d = 2$.

3

The main challenge when constructing a performance curve is the proper selection of K_d''/K_{fs} and K_b/K_{fs} ratios to achieve the desired seismic response reduction. Typically, an increase of the supplemental damping (K_d''/K_{fs}) results into an increase in the number of dampers to be installed. This is expected to increase the total supporting stiffness (K_b). In the present study it is assumed that K_b/K_d'' is constant and equal to 2 as suggested in prior studies [25]. As an example, three possible retrofit scenarios are shown herein, K_d''/K_{fs}=0.25, 0,5 and 1.0, representing low, medium and high damping cases, respectively. The corresponding values for the effective damping and the displacement and force reductions are shown in Figure 4. For instance, for the high damping case, K_d''/K_{fs}=1.0 and K_b/K_{fs}=2.0, the effective damping is 18% and the associated displacement reduction factor, R_d=0.40. This also yields into a force reduction factor of about R_a=0.60.
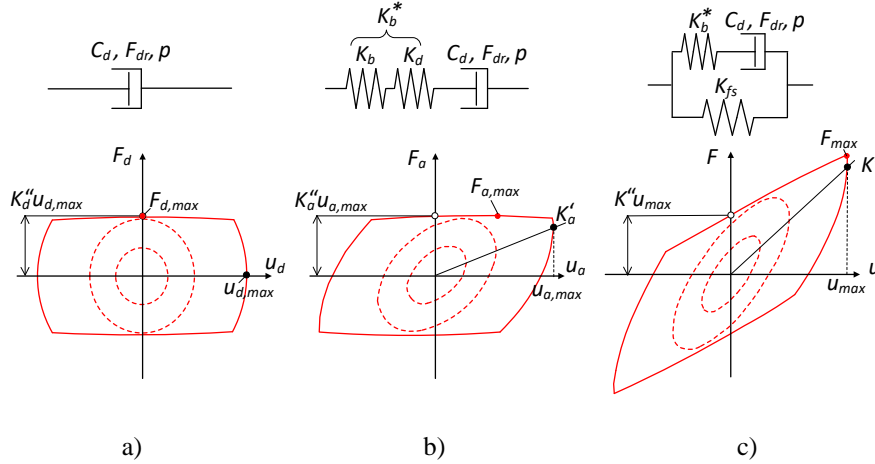

Figure 3. SDF representation of bilinear oil damper models and their force-displacement relations.
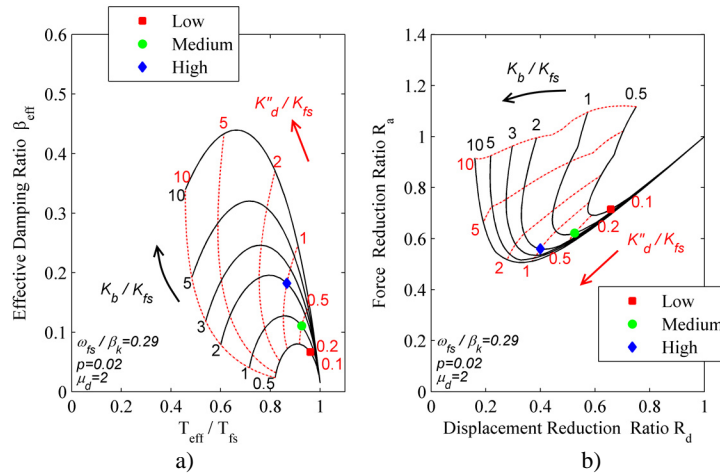

Figure 4: Performance curves of archetype 40-story building equipped with bilinear oil dampers in the Y-loading direction.

Vertical Damping Distribution

Once the key damper design parameters (e.g., K_d''/K_{fs} and K_b/K_{fs} ratios) are determined, the SDF parameters shall be transformed into MDF parameters along the building height. This is done through a vertical damping distribution method. Several methods exist in the literature for this purpose [27; 28]. Three distribution methods are examined herein, namely stiffness, direct shear force and effective shear force proportional damping distribution methods. If dampers are designed according to the first method, the loss stiffness K_d'' will be proportional to the story stiffness of the building to be retrofitted. If the direct shear force proportional method is utilized, the damper's storage stiffness (K_a') within each story becomes directly proportional to the story shear force demand. The above damping distribution methods assume that dampers are provided at all levels. When the effective shear force proportional damping distribution method is employed, dampers are distributed within stories that an additional effective storage stiffness (K') is needed in order to achieve a uniform story drift distribution along a building's height. Detailed formulations on how to distribute supplemental damping based on the aforementioned methods can be found in [21]

Simplified MDF Models

Shear beam models can be utilized for simplified MDF representation of MRF buildings equipped with dampers. This representation may not be adequate for tall buildings because considerable flexural deformations are expected. This is confirmed by sensitivity studies were carried out with different simplified MDF modeling assumptions to compare the seismic demands of interest with an explicit 2D model of the 40-story building. For this reason, it is rational to employ flexural-shear beam models (see Figure 2c). The building properties (e.g., elastic story stiffnesses) are extracted from 2-dimensional lateral load analysis based on a code-based lateral load pattern as per ASCE-7 [29]. In the flexural-shear beam model, the story shear stiffnesses are represented through a translational link element, while flexural stiffnesses are modeled with a rotational link element. The oil dampers are idealized with a *BilinearOilDamper* material model [30]. Details regarding the flexural-shear beam models and the aforementioned sensitivity studies can be found in Akcelyan [21].

Computation of EDPs and development of MDF Performance Curves

A flexural-shear beam model idealization of the prototype building is subjected to a set of 40 ground motions scaled at the BSE-2E seismic intensity. For brevity, results in the Y-direction are presented herein. The solid black lines shown in Figure 5 are the median EDPs of the steel MRF without dampers, in terms of peak story drift ratios (SDRs), peak floor displacements, peak absolute floor accelerations and peak story shear forces. Twenty-three K_d''/K_{fs} values are considered (range: 0.05 to 5.0) for the seismic retrofit. The rest of the parameters are kept constant (i.e., $\mu_d = 2.0$, $p = 0.02$, $\beta_k = 4.5$ and $K_b/K_d'' = 2.0$). Since the effective shear force proportional damping distribution is employed, the peak SDRs along the building height become relatively uniform when the supplemental damping increases. The EDP medians for each one of the 23 cases are shown in blue (SDR and floor displacement) or red (absolute floor acceleration and story shear force) lines in Figure 5. In order to trace the optimal seismic retrofit design solution, the EDPs shown in Figure 5 are transformed into MDF performance curves, which are shown in Figure 6. The variation of peak and average SDR as well as the peak roof displacement with increasing K_d''/K_{fs} ratio is depicted in Figure 6a. The data point corresponding to $K_d''/K_{fs} = 0$ represents the frame without any dampers. At this level, the peak SDRs are larger than 3%. They gradually reduce with increasing K_d''/K_{fs} ratios. The MDF performance curves can help a designer to select the required K_d''/K_{fs} to satisfy an SDR performance target. Figure 6b shows the displacement reduction, R_d that is achieved with respect to a selected retrofit design. When $K_d''/K_{fs} = 0$ (bare frame), then $R_d = 1$ (i.e., there is no reduction). The same figure shows that the peak SDR reduction is more prominent than that in the peak roof drift ratios. Similar graphs are developed for the peak absolute floor acceleration and base shear force demands as shown in Figure 6c. The former is normalized with respect to the acceleration of gravity, g, while the latter with respect to the seismic weight of the building. Referring to Figure 6d, a force-acceleration response reduction of about 40 to 50% can only be achieved for selected K_d''/K_f ratios. Therefore, design scenarios with $K_d''/K_f > 1$ are not optimal. Although the effective shear force proportional damping distribution method can achieve a desired reduction in peak SDRs by providing dampers at certain stories, it is not as efficient in reducing peak absolute floor accelerations in the upper floors of the building. The aforementioned aspects are not typically depicted by SDF-based simplified methods.

CONCLUSIONS

This paper presented the development of a practical tool, called MDF performance curves, for the design of tall buildings with supplemental damping devices. The methodological steps to deploy the tool are discussed through a step-by-step example. This comprises a 40-story steel frame building designed in 1970s and it is retrofitted with bilinear oil dampers. In brief, for a preliminary selection of SDF damper parameters, the performance curves method is utilized for the prototype building. Several vertical damping distribution methods are employed. Flexural-shear beam models idealize the behavior of the prototype building equipped with dampers. Thus, the importance of flexural deformations, which are common in tall buildings, are properly traced. Story-based EDP parameters are obtained based on the above models for a suite of 40 ground motions. The MDF performance curves are constructed based on 23 damper design parameters. Unlike other simplified methods, the proposed MDF performance curves facilitate the quantification of EDPs along a building's height. The tool captures critical aspects of a tall building's behavior (e.g., higher mode effects, flexural deformations and irregular damping distribution). In turn, the seismic retrofit of the 40-story tall building based on multiple strategies can be easily facilitated [26].
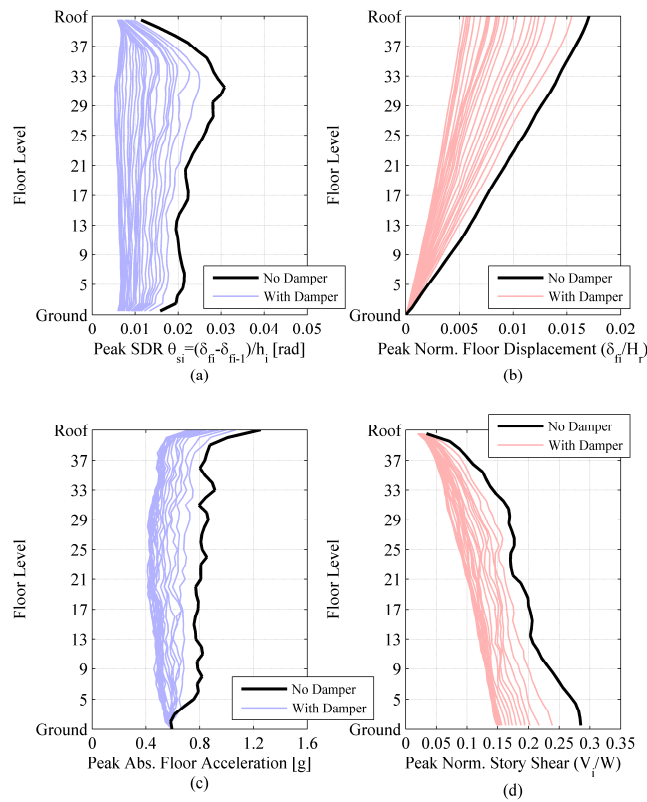
Figure 5. Seismic demands with/without dampers Y-loading direction based on the effective shear force proportional damping distribution.
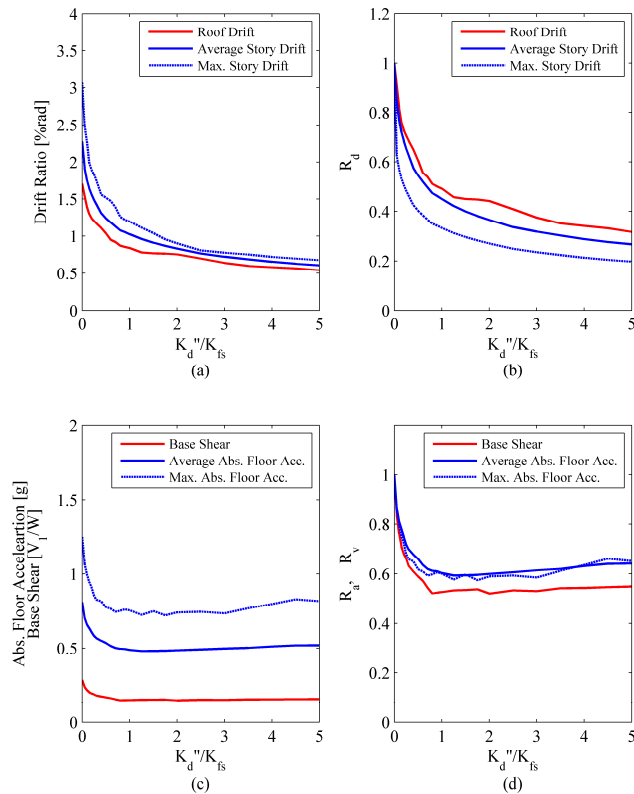

Figure 6. MDF performance curves.

REFERENCES

[1] Christopoulos, C., and Filiatrault, A. (2006). *Principles of supplemental damping and seismic isolation*, IUSS Press, Milan, Italy.

[2] FEMA (1997). "NEHRP provisions for the seismic rehabilitation of buildings." *FEMA 273 (Guidelines) and 274 (Commentary)*, Federal Emergency Management Agency, Washington, D.C.

[3] Akcelyan, S., Lignos, D. G., Hikino, T., and Nakashima, M. (2016). "Evaluation of simplified and state-of-the-art analysis procedures for steel frame buildings equipped with supplemental damping devices based on E-Defense full-scale shake table tests." *Journal of Structural Engineering*, 142(6), 04016024.

[4] Kasai, K., Mita, A., Kitamura, H., Matsuda, K., Morgan, T. A., and Taylor, A. W. (2013). "Performance of seismic protection technologies during the 2011 Tohoku-Oki Earthquake." *Earthquake Spectra*, 29(S1), S265-S293.

[5] Kasai, K., Lu, X., Pu, W., Yamashita, T., Arakawa, Y., and Zhou, Y. (2013). "Effective retrofit using dampers for a steel tall building shaken by 2011 East Japan Earthquake: China-Japan cooperation program (Part 2)." *Proc., 10th International Conference on Urban Earthquake Engineering (10CUEE)*, Tokyo Institute of Technology, Tokyo, Japan.

[6] Hwang, J., Huang, Y., Yi, S., and Ho, S. (2008). "Design formulations for supplemental viscous dampers to building structures." *Journal of Structural Engineering*, 134(1), 22-31.

[7] Ishii, M., and Kasai, K. (2010). "Shear spring model for time history analysis of multi-story passive controlled buildings." *J. Struct. Constr. Eng.*, 75(647), 103-112.

[8] Guo, J. W. W., and Christopoulos, C. (2013). "Performance spectra based method for the seismic design of structures equipped with passive supplemental damping systems." *Earthquake Engineering & Structural Dynamics*, 42(6), 935-952.

[9] Hutt, C. M., Almufti, I., Willford, M., and Deierlein, G. (2016). "Seismic loss and downtime assessment of existing tall steel-framed buildings and strategies for increased resilience." *Journal of Structural Engineering*, 142(8), C4015005.

[10] ICBO (1973). "Uniform Building Code (UBC)." International Conference of Building Officials, Washington, DC.

[11] McKenna, F. T. (1997). "Object-oriented finite element programming: frameworks for analysis, algorithms and parallel computing." Ph.D. Dissertation, University of California, Berkeley.

[12] ASCE/SEI (2014). "Seismic evaluation and retrofit of existing buildings." *ASCE/SEI 41-13*, American Society of Civil Engineers, Reston, VA.

[13] Elkady, A., and Lignos, D. G. (2018). "Full-scale testing of deep wide-flange steel columns under multiaxis cyclic loading: loading sequence, boundary effects, and lateral stability bracing force demands." 144(2), 04017189.

[14] Elkady, A., and Lignos, D. G. (2018). "Improved seismic design and nonlinear modeling recommendations for wide-flange steel columns." 144(9), 04018162.

[15] Kostic, S. M., and Filippou, F. C. (2012). "Section discretization of fiber beam-column elements for cyclic inelasticresponse." 138(5), 592-601.

[16] Ibarra, L. F., and Krawinkler, H. (2005). *Global collapse of frame structures under seismic excitations*, Pacific Earthquake Engineering Research Center.

[17] Lignos, D. G., and Krawinkler, H. (2011). "Deterioration modeling of steel components in support of collapse prediction of steel moment frames under earthquake loading." *Journal of Structural Engineering*, 137(11), 1291-1302.

[18] Lignos, D., Hartloper, A. R., Elkady, A. M. A., Hamburger, R., and Deierlein, G. "Revised ASCE-41 modeling recommendations for moment-resisting frame systems." *Proc., Proceedings of the 11th US National Conference on Earthquake Engineering (11NCEE)*.

[19] Krawinkler, H. (1978). "Shear in beam-column joints in seismic design of steel frames." *Engineering Journal*, 15(3), 82-91.

[20] Gupta, A., and Krawinkler, H. (1999). "Seismic demands for the performance evaluation of steel moment resisting frame structures." Ph.D. Dissertation, Stanford University.

[21] Akcelyan, S. (2017). "Seismic retrofit of existing steel tall buildings with supplemental damping devices." Ph.D. Dissertation, McGill University.

[22] Kasai, K., Nakai, M., Nakamura, Y., Asai, H., Suzuki, Y., and Ishii, M. (2008). "Current status of building passive control in Japan." *Proc., The 14th World Conference on Earthquake Engineering*, Beijing, China.

[23] Kasai, K., and Matsuda, K. (2014). "Full-scale dynamic testing of response-controlled buildings and their components: concepts, methods, and findings." *Earthquake Engineering and Engineering Vibration*, 13(1), 167-181 English.

[24] Fu, Y., and Kasai, K. (1998). "Comparative study of frames using viscoelastic and viscous dampers." *Journal of Structural Engineering*, 124(5), 513-522.

[25] Kasai, K., Ito, H., and Ogura, T. (2008). "Passive control design method based on tuning of equivalent stiffness of bilinear oil dampers." *Journal of structural and construction engineering*, 73(630), 1281-1288.

[26] Akcelyan, S., and Lignos, D. "Seismic retrofit of steel tall buildings with bilinear oil dampers." *Proc., 16th European Conference on Earthquake Engineering*.

[27] Whittle, J. K., Williams, M. S., Karavasilis, T. L., and Blakeborough, A. (2012). "A comparison of viscous damper placement methods for improving seismic building design." *Journal of Earthquake Engineering*, 16(4), 540-560.

[28] Hwang, J.-S., Lin, W.-C., and Wu, N.-J. (2013). "Comparison of distribution methods for viscous damping coefficients to buildings." *Structure and Infrastructure Engineering*, 9(1), 28-41.

[29] ASCE (2010). "Minimum design loads for buildings and other structures." *ASCE/SEI 7-10*, American Society of Civil Engineers, Reston, VA.

[30] Akcelyan, S., Lignos, D. G., and Hikino, T. (2018). "Adaptive numerical method algorithms for nonlinear viscous and bilinear oil damper models subjected to dynamic loading." *Soil Dynamics and Earthquake Engineering*, 113, 488-502.